

Article

Combination of Engineered Expression of Polysialic Acid on Transplanted Schwann Cells and in Injured Rat Spinal Cord Promotes Significant Axonal Growth and Functional Recovery

Fangyou Gao ^{1,†,‡}, Yi Zhang ^{1,†}, Dongsheng Wu ¹, Juan Luo ^{1,§}, Svetlana Gushchina ^{1,2} and Xuenong Bo ^{1,*} 

¹ Centre for Neuroscience, Surgery and Trauma, Faculty of Medicine and Dentistry, Queen Mary University of London, London E1 2AT, UK; gaofangyou@gz5055.com (F.G.); yi.zhang@qmul.ac.uk (Y.Z.); dong.wu@qmul.ac.uk (D.W.); juanluo@hust.edu.cn (J.L.); s.gushchina@qmul.ac.uk (S.G.)

² Department of Cytology, Histology and Embryology, Ogarev Mordovia State University, Saransk 430005, Russia

* Correspondence: x.bo@qmul.ac.uk; Tel.: +44-20-78822294

† These authors contributed equally to this work.

‡ Current address: Department of Neurosurgery, Guizhou Provincial People's Hospital, Guiyang 550002, China.

§ Current address: Department of Physiology, Tongji Medical College, Huazhong University of Science and Technology, Wuhan 430030, China.

Abstract: Providing cellular support and modifying the glial scar around the lesion are two key strategies for promoting axonal regeneration after spinal cord injury. We showed previously that over-expressing polysialic acid (PSA) on Schwann cells (SCs) by lentiviral vector (LV)-mediated expression of polysialyltransferase (PST) facilitated their integration and migration in the injured spinal cord. We also showed that PSA over-expression in the injured spinal cord modified the glial scar and promoted the growth of ascending sensory axons. In this study, we combined the PST/SC transplantation with LV/PST injection in spinal cords after dorsal column transection and found the combined treatments led to faster and more profound locomotor functional recovery compared with animals receiving combined GFP/SC transplantation with LV/GFP injection. Histological examination showed significantly more injured corticospinal axons growing close to the lesion/transplant borders and into the caudal spinal cord in the PST group than in the GFP group. We also found over-expressing PSA around the lesion site did not cause allodynia and hyperalgesia in our injury model. These results demonstrate the promising therapeutic benefit of over-expressing PSA in transplanted SCs and spinal cord in promoting axonal growth and restoring motor function.

Keywords: spinal cord injury; polysialic acid; Schwann cell; transplantation; corticospinal axon; axonal regeneration



Citation: Gao, F.; Zhang, Y.; Wu, D.; Luo, J.; Gushchina, S.; Bo, X. Combination of Engineered Expression of Polysialic Acid on Transplanted Schwann Cells and in Injured Rat Spinal Cord Promotes Significant Axonal Growth and Functional Recovery. *Neuroglia* **2023**, *4*, 222–238. <https://doi.org/10.3390/neuroglia4040016>

Academic Editor: Jan Kaslin

Received: 7 August 2023

Revised: 14 September 2023

Accepted: 18 September 2023

Published: 23 September 2023



Copyright: © 2023 by the authors. Licensee MDPI, Basel, Switzerland. This article is an open access article distributed under the terms and conditions of the Creative Commons Attribution (CC BY) license (<https://creativecommons.org/licenses/by/4.0/>).

1. Introduction

Injury to the spinal cord results in progressive cell death, formation of cavities, transection of long axon tracts, axonal demyelination, and glial scar formation around the lesion site [1]. Cell transplantation is a promising strategy for the repair of the injured central nervous system (CNS) [2,3]. Cells transplanted into the injury site may replace lost cells and provide a permissive substrate for axonal growth. Cellular transplantation can also ameliorate the glial scar. Schwann cells (SCs) have been used for grafting into the injured spinal cord in animal experiments for many years as they can be obtained easily and can myelinate CNS axons [4,5], which is crucial for functional recovery. Phase I clinical trials conducted on autologous human SC transplantation into the injured spinal cords showed this procedure was safe [6–9], which has paved the way for further clinical trials. Previous animal experiments showed that naïve SCs do not mingle well with CNS glial cells and do not migrate into the host tissue as they are the myelinating cells for peripheral nerves [10].

Such interaction between SCs and CNS tissues significantly limits their success in promoting axon regeneration, as axons do not grow beyond the SCs transplants. Following spinal cord injury, glial cells, particularly astrocytes, undergo hypertrophy and proliferate to form a glial scar around the lesion cavity [11]. The glial scar formed around the lesion site acts as both a physical and a biological barrier for axonal regeneration and migration of transplanted cells [12]. In contrast to the upregulation of inhibitory molecules, polysialic acid (PSA), a permissive molecule for axonal growth and cell migration, is also temporarily upregulated by a subpopulation of astrocytes in the glial scar [13,14]. The re-expression of PSA in the glial scar is temporally and spatially correlated with axonal sprouting [13,14].

PSA is a linear homopolymer of α -2,8-linked sialic acid residues and is mainly attached to neural cell adhesion molecules (NCAMs). PSA is highly expressed in the nervous system during development. By modulating the adhesive property of NCAM, PSA is implicated in many neural morphogenic events, including cell migration, axonal guidance, and the formation of terminal arbores [15,16]. In the adult brain, PSA expression is mainly restricted to regions with a relatively high degree of structural plasticity, such as the olfactory bulb, hippocampus, and hypothalamus [17,18]. Such a growth-facilitating property of PSA can be explored for neural repair [19,20]. Polysialyltransferases ST8SiaIV (PST) and ST8SiaII (STX) are two enzymes that attach PSA chains to NCAM [21,22]. We have previously used a lentiviral vector carrying the PST gene (LV/PST) to transduce spinal cord cells *in vivo* and demonstrated the effectiveness of the engineered expression of PSA in the injured spinal cord in promoting sensory axonal regeneration [23,24]. A similar axonal growth-promoting effect was also reported by El Maarouf et al. [25]. Engineered expression of PSA in the glial scar around the CNS lesion site can alter the structure of the glial scar and render it permissive for axonal growth. We and other labs also showed that the engineered expression of PSA on SCs is able to enhance the migratory potential of SCs *in vitro* and *in vivo* [10,26–28]. Transplantation of PSA-expressing SCs has been shown to enhance axonal growth and boost functional recovery following spinal cord injury in rats and mice [28,29]. Furthermore, we also showed that engineered expression of PSA in and around the lesion site could further enhance the migration and integration of SCs into host tissue [10]. In this study, we combined the transplantation of PST-transduced SCs into the lesion with the engineered expression of PSA by direct injection of LV/PST around the lesion site to modify the glial scar after the dorsal column transection of the rat spinal cord. We postulate that the expression of PSA in the spinal cord could render the glial scar permissive for the regeneration and sprouting of corticospinal tract (CST) axons while the PST-transduced SCs would form a bridge to support CST axonal growth, leading to motor functional recovery. We also examined the effects of PSA expression on pain sensitivity associated with the potential sprouting of primary afferent sensory nerves. We found that the combinatory treatment of PST-SC transplantation with PSA over-expression in injured spinal cord significantly promoted motor functional recovery compared with the transplantation of GFP-SCs with intraspinal GFP expression, and also markedly enhanced corticospinal axon growth and sprouting into the grey matter caudal to the lesion. The results indicate that combining PST-SC transplantation and engineered PSA expression around spinal cord lesions is a more effective approach in promoting CST axon regeneration and sprouting.

2. Materials and Methods

2.1. Production of Lentiviral Vectors and Transduction of Schwann Cells

Mouse PST cDNA was kindly provided by M. Eckhardt [21] and subcloned into the lentiviral transfer vector pRRL. In order to directly visualize the expression and localization of PST in transduced cells, PST cDNA was fused to the N-terminal of GFP cDNA to generate PST-GFP. The fusion of GFP to the C-terminal of PST does not interfere with its enzymatic activity [30]. For control, GFP cDNA was also subcloned into the pRRL vector. Self-inactivating lentiviral vectors (LV) were made by co-transfecting HEK293T cells using a three-plasmid system [31]. The lentiviral vector carrying the PST-GFP fusion

construct is referred to as LV/PST. Lentiviral particles were concentrated by ultracentrifugation. The titers were determined by the transduction of HEK293 cells using serially diluted viral stocks. The titer for LV/PST was in the range of $0.5\text{--}1 \times 10^{10}$ TU/mL, and $1\text{--}7 \times 10^{10}$ TU/mL for LV/GFP.

SCs were isolated from the sciatic nerves and brachial plexus of Wistar rats of postnatal day 2, as described previously [32]. Nerves were cut into small pieces and cells were dissociated after trypsin treatment, followed by filtration through a 70 μm cell strainer and centrifugation at $100 \times g$ for 10 min. Cells were plated into a PDL-coated 35 mm dish with DMEM containing 10% fetal bovine serum (FBS), 100 I.U./mL penicillin and 100 $\mu\text{g}/\text{mL}$ streptomycin, and 10 μM cytosine arabinoside to inhibit the growth of fibroblasts. Two days later, the medium was replaced with a specially formulated SC culture medium, which stimulated the division of the Schwann cells. The SC medium is composed of DMEM, 10% FBS, 25 ng/mL β -heregulin (R&D Systems), 2 μM forskolin (Sigma-Aldrich, Poole, UK), 25 ng/mL fibroblast growth factors (PeproTech EC Ltd., London, UK), 5 $\mu\text{g}/\text{mL}$ insulin (Sigma-Aldrich), and 100 I.U./mL penicillin and 100 $\mu\text{g}/\text{mL}$ streptomycin (Sigma-Aldrich). The purity of all primary SC cultures was evaluated by immunostaining for SC markers p75 neurotrophin receptor (p75^{NTR}) and S100. Highly purified cultures (>95% SCs), up to three passages, were used in all experiments. SCs transduced with LV/GFP are referred to as GFP/SCs. Due to weak GFP fluorescence from PST-GFP fusion proteins expressed in transplanted PST/SCs, PST/SCs were co-transduced with LV/GFP for easy identification. The efficiency of co-transduction was $95 \pm 2\%$. The co-transduced cells will be referred to as GFP-PST/SCs.

2.2. Animal Surgery

All animal work was performed in accordance with the Animals (Scientific Procedures) Act 1986 of the UK and covered by the project and personal licenses issued by the Home Office. All efforts were made to minimize animal use and suffering. Adult female Wistar rats (200–250 g) were used for this study. Rats were group-housed in standard cages with free access to food and water and kept on a 12-h light/dark cycle. All surgery was performed under isoflurane anesthesia and conducted using aseptic techniques. The segment of the 8th thoracic (T8) spinal cord was exposed by a laminectomy under an operating microscope. The dura was opened, and the dorsal column was cut bilaterally using microsurgical scissors to a depth of 1.5 mm, which led to complete transection of the ascending proprioception tract, dorsal column medial lemniscus, and the main dorsal CST tract located in the ventral portion of the dorsal column. The animals were divided into two groups (7 per group): one group received GFP-PST/SC transplantation and LV/PST injection (PST group) and the other group received GFP/SC transplantation and LV/GFP injection (GFP group). Each animal was placed in a stereotactic frame, and 1 μL of LV/PST or LV/GFP (containing 1×10^6 TU of LV/PST or LV/GFP) was slowly injected into the rostral and caudal margin of the lesion site at 1 mm left and right of midline, respectively. This was carried out using a removable 33-gauge needle attached to a Hamilton syringe, at a depth of 1 mm below the surface of the spinal cord at a speed of 200 nL/min [23]. A amount of 1.5×10^6 SCs in 6 μL DMEM was injected into the lesion site. A small piece of fibronectin flak (Sigma-Aldrich) was used to cover the surface of the transplants and adjacent spinal cord. After surgery, the muscle and skin incisions were closed in separate layers with sutures. The animals were treated with cyclosporine (10 $\mu\text{g}/\text{g}$ body weight) subcutaneously before surgery and daily for the first two weeks after surgery. Normal saline equivalent to 2% of body weight was administered intraperitoneally immediately after surgery and then subcutaneously for the first 3 days after surgery. Analgesia was provided by subcutaneous injection of buprenorphine immediately following anesthesia and 24 h post-surgery. Rats were culled if they displayed rapid weight loss or any signs of lethargy or distress.

Following spinal cord surgery, the function of the descending motor system was assessed behaviorally. Six weeks after surgery, 1 μL of 10% biotinylated dextran amine

(BDA, MW 10,000, Thermo Fisher Scientific UK, Dartford, UK) was injected bilaterally into each of the 6 sites in either motor cortex to trace CST axons. The rats were anaesthetized and fixed in a stereotactic frame. The skull was exposed and injections were made at a depth of 2 mm dorsoventrally into the motor cortex region: AP -1.5 mm, L 2.5 mm; AP -0.5 mm, L 3.5 mm; AP $+0.5$ mm, L 3.5 mm; AP $+1.0$ mm, L 1.5 mm; AP $+1.5$ mm, L 2.5 mm; AP $+2$ mm, L 3.5 mm (in reference to bregma: AP, anterior–posterior; L, lateral) [33]. Nine weeks after spinal cord injury, animals were sacrificed with a lethal intraperitoneal injection of pentobarbitone sodium and transcardially perfused with saline, followed by 4% paraformaldehyde. Segments of the spinal cord containing the lesion site and a small segment from the cervical spinal cord C4 and the lumbar spinal cord L4 were removed. Subsequently, they were postfixed in 4% paraformaldehyde overnight, cryoprotected with 30% sucrose in 0.1 M phosphate buffer, and then embedded in OCT compound.

2.3. Immunohistochemistry

For detection of PSA expression in GFP/SCs and PST/SCs, SCs were fixed with 4% paraformaldehyde 7 d after infection of the cultured SCs with LV/GFP or LV/PST + LV/GFP and blocked with 10% normal donkey serum in phosphate buffered saline (PBS). Mouse monoclonal antibody against PSA (IgM, 5A5, 1:200, Hybridoma Bank, Iowa City, IA, USA) was applied to the SCs overnight at 4 °C, followed by incubation with Cy3-conjugated donkey anti-mouse IgM at room temperature for 2 h. For nucleus staining, 4',6'-diaminidino-2-phenylindole (DAPI, 0.0002%) was applied for 5 min.

The segments of spinal cords containing the lesion site were cut horizontally at 15 μ m thickness on a cryostat, and serial sections extending the whole lesion area were collected on 4 sets of slides. The C4 and L4 spinal cord segments were cut transversely, the C4 sections were stained for BDA to check the efficiency of BDA tracing, and the L4 sections were immunostained for protein kinase C gamma (PKC γ) to examine the completeness of dorsal CST transection. Sections were blocked in 10% normal donkey serum in 0.1M Tris buffered saline with 0.05% Tween 20 for 2 h. PKC γ was immunostained with a rabbit polyclonal IgG (1:250, Santa Cruz Biotechnology Inc., Santa Cruz, CA, USA). For BDA labelling, sections were incubated in avidin biotin peroxidase complex (Vector Laboratories, Peterborough, UK) overnight, followed by incubation with tyramide Cy3 (1:100, PerkinElmer Life and Analytical Sciences, Waltham, MA, USA) for 10 min at room temperature. For PSA and glial fibrillary acidic protein (GFAP) immunostaining, selected sections were incubated with antibodies against PSA (5A5, 1:200) or GFAP (mouse monoclonal IgG, 1:1000, Sigma-Aldrich) overnight, followed by incubation with appropriate secondary antibodies (Cy3-conjugated donkey anti-mouse IgM, or AMCA-conjugated donkey anti-mouse IgG, Jackson ImmunoResearch Laboratories, West Grove, PA, USA) at 1:400 for 2 h. For immunostaining of peripheral myelin protein P0, the sections were pre-treated with ice-cold methanol for 5 min before being incubated with the blocking buffer. They were then incubated with a mouse monoclonal IgG against P0 protein (1:3000, a gift from Astex Therapeutics, Cambridge, UK) and a polyclonal rabbit IgG against neurofilament 200 (NF200, 1:1000, Sigma-Aldrich) overnight. The sections were subsequently incubated with a mixture of appropriate secondary antibodies (Cy3-conjugated donkey-anti-mouse IgG and Cy5-conjugated donkey-anti-rabbit IgG) for 2 h. Sections were mounted in a mixture of glycerol and PBS (9:1) containing 2.5% DAPCO (Sigma-Aldrich) and coverslipped. Sections were viewed under a Leica epifluorescence microscope or a Zeiss confocal microscope.

2.4. Behavioral Assessment

Locomotor impairments of the rats after spinal cord injury were assessed using a 120-cm long horizontal ladder-walking test. Animals were trained for two weeks before surgery. The first test was performed 3 days after surgery and then weekly for 9 weeks. Animals were videotaped, and the total number of hindlimb steps made and the number

of slips were recorded. The data were presented as mean \pm SEM. Two-way ANOVA with post-hoc Tukey tests was performed to analyze the difference between PST and GFP groups.

To assess the effects of spinal cord injury and the over-expression of PSA on pain sensitivity, we used the manual Von Frey (VF) test for mechanical withdrawal thresholds and the Hargreaves test for noxious thermal sensitivity [34]. For the VF test, two baseline measurements of hindpaw reflex sensitivity to punctuate static mechanical stimuli using graded VF nylon filaments were recorded [35]. VF filaments were applied in ascending order to the mid-plantar surface of the hindpaws with a minimum interval of 1 min. The lowest force leading to at least three withdrawals in five trials was defined as the withdrawal threshold to mechanical stimuli. For the Hargreaves test, the time taken for a radiant heat source to elicit a flexion reflex was recorded. Each paw was tested three times and averaged to obtain the mean withdrawal latency. Assessments were performed once a week and up to 9 weeks post-surgery. All the animals were coded, and the behavioral functions were blindly tested by two researchers who were not involved in the microsurgery.

2.5. Image Analysis

For quantification of BDA-labelled CST axons, axons were counted in 12 horizontal sections at 60 μ m intervals from each rat. The number of BDA-labelled axons that intersected the three virtual lines marking the distances from the lesion was counted. The three distance points are illustrated in following figures: 8 mm and 0.9 mm to the rostral lesion border, and 4 mm to the caudal lesion border. Intact dorsolateral CST axons running in the lateral funiculus at the level of the lesion center were also counted and shown as spared CST axons. BDA⁺ axons in the grey matter 20 mm to the caudal lesion border were counted in 4 randomly selected sections. The data were presented as mean \pm SEM. One-way ANOVA with post-hoc Tukey tests was performed to analyze the differences between PST and GFP groups.

3. Results

3.1. Lentiviral PST Gene Transfer Induces PSA Expression In Vitro and In Vivo

PSA immunoreactivity (PSA-ir) was hardly detectable in naïve SCs and GFP/SCs (Figure 1A). In contrast, PST/SCs displayed strong PSA-ir on the cell membrane of the unpermeabilized cells (Figure 1B). In order to define the time window of PSA expression by grafted PST/SCs, we analyzed animals receiving either GFP/SCs or PST/SCs at 1, 4, and 9 weeks after transplantation. PSA-ir was found on many PST/SCs at 1 week after grafting (Figure 1C), to a lower level at 4 weeks (Figure 1D), and only appeared on some cells at 9 weeks (Figure 1E). PSA-ir was not visible on the grafted GFP/SCs.

To study the lentiviral vector-mediated PSA expression in a spinal cord injury model, both the ascending sensory dorsal column medial lemniscus tract and the major dorsal CST were axotomized by dorsal column transection. The site of the lesion, viral vector injection, and the SC transplant are illustrated in Figure 2A. Previously we have shown that injection of LV/GFP into the spinal cord transduced astrocytes, oligodendrocytes, and microglia as well as neurons around the lesion site [23]. Dorsal column transection plus LV/GFP injection induced a moderate up-regulation of PSA-ir around the lesion site 6 weeks after injection [24]. In the current study, PSA-ir was hardly visible 9 weeks after dorsal column transection plus GFP/SC transplantation and LV/GFP injection (Figure 2B). However, injection of LV/PST resulted in the dense and widespread expression of PSA rostral and caudal to the lesion and SC transplant site, and the expression remained high 9 weeks after operation (Figure 2C). Therefore, PSA expression in transplanted SCs is down-regulated significantly 9 weeks after transplantation, while LV/PST injection into the spinal cord is capable of inducing lasting PSA expression around the lesion site.

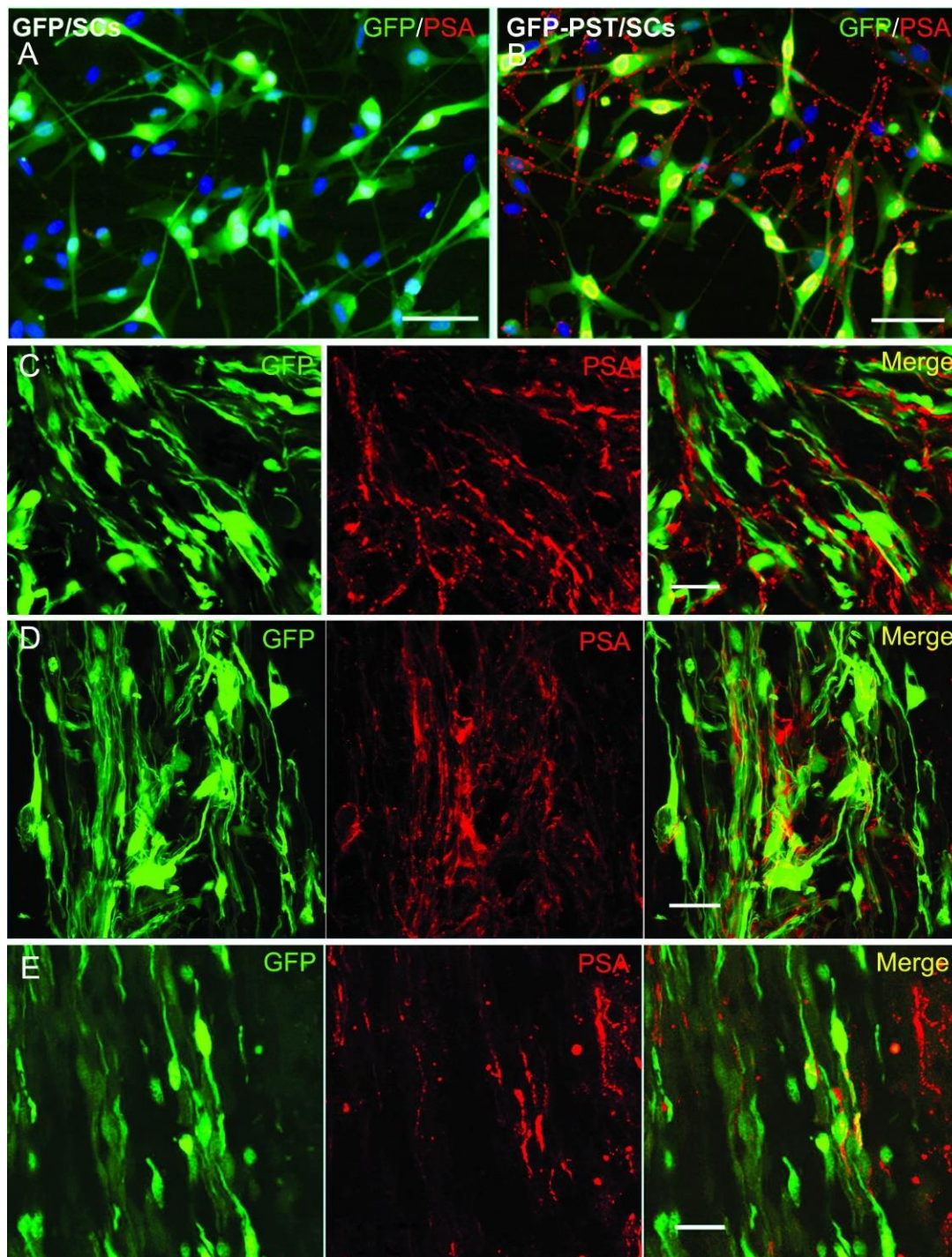


Figure 1. Lentiviral vector-mediated expression of PSA on Schwann cells in vitro and in vivo. (A) Primary Schwann cells (SCs) transduced with LV/GFP: PSA-immunoreactivity (red) was not detectable in LV/GFP-transduced SCs. (B) Primary SCs transduced with both LV/PST and LV/GFP: high-level PSA (red) expression on cell bodies and their processes. The nuclei of SCs were stained with DAPI (blue). In vivo expression of PSA on the LV/PST and LV/GFP co-transduced SCs at 1 week (C), 4 weeks (D), and 9 weeks (E) after grafting into normal rat spinal cord. Scale bar = 50 μm in (A,B), 20 μm in (C–E).

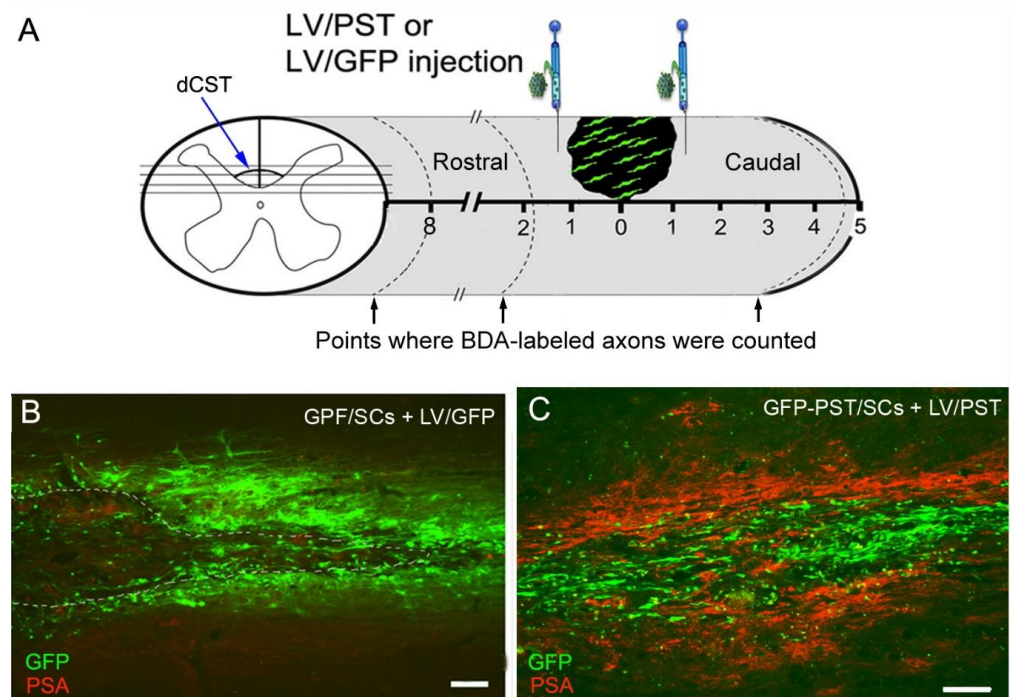


Figure 2. Expression of GFP and PSA in the spinal cord after Schwann cell transplantation and lentiviral vector injection. (A) Schematic illustration of Schwann cell (SC) transplantation and lentiviral vector injection into rat spinal cord in a T8 level dorsal column transection model. dCST: dorsal corticospinal tract. (B) GFP expression in a horizontal spinal cord section 9 weeks after GFP/SCs transplantation plus LV/GFP injection (the lesion is outlined by dashed lines). The majority of GFP⁺ cells around the lesion are LV/GFP-transduced spinal cord cells. (C) PSA expression in a horizontal spinal cord section 9 weeks after transplantation of GFP and PST co-transduced SCs (GFP-PST/SCs) plus LV/PST injection. Green fluorescence shows the transplanted SCs. Scale bar = 100 μ m.

3.2. Combining PST/SC Transplantation with LV/PST Injection Enhances the Growth of Corticospinal Tract Axons

Dorsal column transection injures the major CST axons in the dorsal column but spares the minor components of CST axons running in the dorsolateral and ventral white matter. Complete transection of dorsal CST was verified by examining sequential sections of the spinal cord containing the injury site and further confirmed by the absence of PKC γ -ir in the CST area in the dorsal column in the L4 lumbar segment. CST axons were traced by cortical injection of BDA. In the GFP group, the majority of BDA⁺ axons formed terminal bulbs before they reached the lesion and SC transplants (Figure 3A, enlarged in Panel a, and Figure 4A), while in the PST group, BDA⁺ axons were seen much closer to the transplants and lesion site (Figure 3B). On average, axons terminated 785 ± 101 μ m from the lesion site in the GFP group in comparison with 156 ± 24 μ m in the PST group ($p < 0.001$). There were only a few BDA⁺ axons visible at the rostral borders of the GFP/SC transplants (Figure 3A, enlarged in Panel c). In contrast, in the PST group, many BDA⁺ axonal sprouts were seen at the rostral border of the lesion and SC transplants (Figure 3B, enlarged in Panel b*, which was from an adjacent section). Some BDA⁺ axonal sprouts were seen growing at the interface between the PST/SC transplant and the host tissues and into the grey matter caudal to the lesion site (Figure 3B, enlarged in Panel c and d). In the grey matter caudal to the lesion site, many BDA⁺ axonal profiles with multiple branches and varicose in appearance were found (Figure 3B, Panel f*, from a different section), and these spouting axons might come from intact dorsolateral CST running in the lateral funiculus, as shown in Figure 3B, Panel e*. Although significant axonal growth and sprouting were seen close to the GFP-PST/SC transplants, BDA⁺ axonal sprouts were rarely deep inside the transplants.

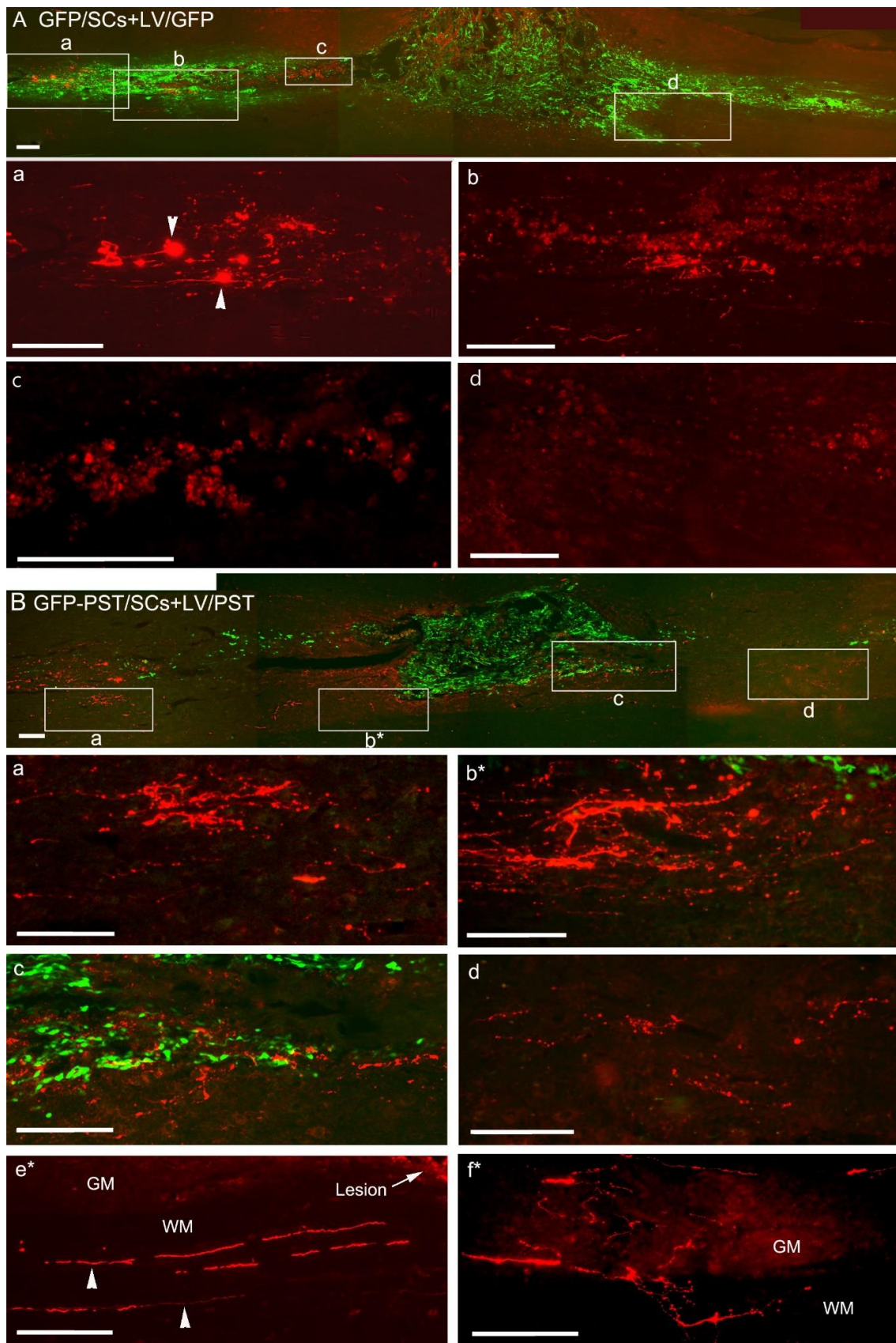


Figure 3. Response of corticospinal tract axons to combined Schwann cell transplantation and engineered GFP or PSA expression in the injured spinal cord. Corticospinal tract axons were labelled

with biotinylated dextran amine (BDA). **(A)** BDA-labelled axons (red) in horizontal spinal cord section from a rat receiving GFP/SCs transplantation plus intraspinal LV/GFP injection. Boxed areas in **(A)** are enlarged in the corresponding image panels (a)–(d) to illustrate the BDA-labelled axons. Panel (a) and (b) show that many BDA⁺ axons formed end bulbs (arrowheads) before reaching the lesion/transplant. Note that axon end bulbs looked much bigger than they should have been due to strong fluorescence at the end bulbs causing halation in the photomicrograph. BDA⁺ axonal profiles were hardly visible immediately rostral to the lesion border and around transplant (c) and (d). The red fluorescent structures close to the lesion site were auto-fluorescent cell debris. **(B)** BDA-labelled axons (red) in horizontal spinal cord section from a rat receiving transplantation of GFP and PST co-transduced SCs (GFP-PST/SCs) plus LV/PST injection. Boxed areas (a), (c), and (d) in **(B)** are enlarged in corresponding panels (a), (c), and (d) to illustrate the BDA-labelled axons. (b*) is from an adjacent section to **(B)** corresponding to the boxed area b* in **(B)**. Numerous BDA⁺ axonal sprouts were present at the rostral spinal cord (a) and close to the PST/SC transplant (b,c). Some BDA⁺ axons penetrated the distal spinal cord (d). Panel (e*) shows the BDA-labelled intact lateral CST axons (arrowheads) in the white matter (WM) from the same section as (b*). GM, grey matter. Panel (f*) shows an image taken from a different animal illustrating numerous BDA⁺ axonal profiles of varicose appearance sprouting in the grey matter in the distal spinal cord. Scale bar = 200 μ m.

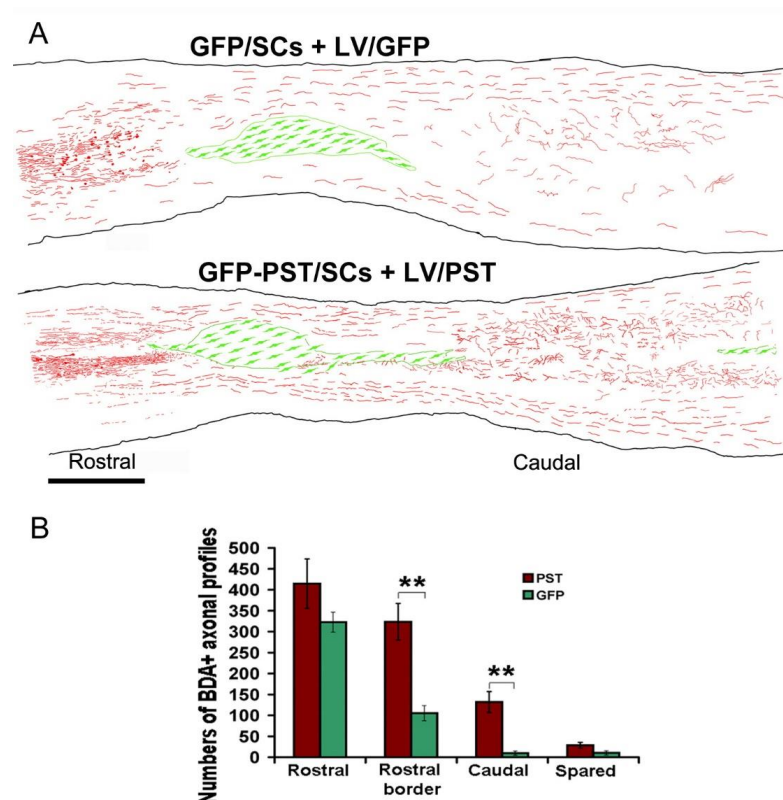


Figure 4. BDA-labelled axonal profiles in spinal cord sections after combined Schwann cell transplantation and engineered GFP or PSA expression. **(A)** Composite figures by camera lucida drawing showing the distribution of BDA-labelled corticospinal tract axons and their orientation relative to the lesion site in four horizontal sections from a rat in the GFP group and a rat in the PST group. BDA⁺ axonal profiles are shown in red and Schwann cells in green. The outline of the spinal cord and the transplants were traced from a single section close to the center of the spinal cord. The BDA⁺ axons from the other three sections were superimposed onto the first section. Scale bar = 1 mm. **(B)** Quantification of BDA⁺ axonal profiles at different levels of the spinal cord. The number of BDA⁺ axons was counted in three distance points, as illustrated in Figure 2A: 8 mm (Rostral) and 0.9 mm (Rostral border) rostral to the lesion border, and 4 mm caudal to the lesion border (Caudal). The numbers of BDA⁺ axonal profiles were counted from 12 horizontal sections at 60 μ m intervals. Values are expressed as mean \pm SEM. ** $p < 0.01$, one-way ANOVA, $n = 7$.

As many of the weakly BDA-labelled axons, especially those thin axonal sprouts, were difficult to see clearly in the montaged images (Figure 3A,B), composite figures of camera lucida drawings based on four sections from one rat in the GFP group and one from the PST group were generated to provide a direct view of the BDA-labelled axonal profiles (Figure 4A). It is evident that many more BDA-labelled axonal profiles were present close to the rostral lesion border and in the grey matter caudal to the lesion. Quantification of BDA⁺ axonal profiles shows that there was no significant difference in the numbers of BDA⁺ axons at 8 mm rostral to the lesion border, indicating the BDA labelling efficiency was similar between the two groups. However, there were significantly more BDA⁺ axons at the rostral border in the PST group than that in the GFP group (324 ± 44 vs. 105 ± 18 , $p < 0.01$) (Figure 4B). Similarly, there were significantly more BDA⁺ axonal profiles at 4 mm caudal to the lesion border in the PST group than in the GFP group (132 ± 25 vs. 10 ± 5 , $p < 0.01$). To evaluate the sprouting axons further caudal to the lesion, we counted the BDA⁺ axons in the grey matter 20 mm caudal to the lesion border from four randomly chosen sections: 20 ± 4 axons were counted in the PST group and 1 ± 1 in the GFP group. The numbers of spared axons in the lateral funiculus at the level of the lesion center were not significantly different between the two groups (PST group: 29 ± 7 vs. GFP group: 10 ± 5 , $p > 0.05$) (Figure 4B). Pearson correlation test shows that the numbers of BDA⁺ axonal profiles in the caudal spinal cord are closely correlated with the number of spared BDA⁺ axons ($r = 0.98$, $p = 0.001$) in the GFP group, but are not correlated in the PST group ($r = 0.687$, $p = 0.132$), indicating that a proportion of the BDA⁺ axons in the PST group was regenerating CST axons.

3.3. Combining PST/SC Transplantation with LV/PST Injection Promotes Locomotor Functional Recovery

Horizontal ladder crossing was used to assess the hindlimb function of the rats. After being trained for 2 weeks, animals crossed the ladder without any foot slip. Three days after dorsal column transection at T8 level, animals crossed the ladder by pulling their hindlimbs or refused to cross the ladder, which was recorded as maximum foot slips. One week after injury, the locomotor function of the hindlimbs in both PST and GFP groups started to improve (Figure 5A). The rats in the PST group showed a tendency for a faster and greater degree of recovery than those in the GFP group in the first three weeks after injury. By the fourth week, rats in the PST group showed significantly improved hindlimb performance compared with those in the GFP group, followed by a further gradual improvement until the end of the experiment at 9 weeks after injury. The GFP group recovered at a slower rate and also to a lesser degree compared with the PST group (Figure 5A). The difference in the degrees of locomotor functional recovery between the PST and the GFP groups remained significant from 4 weeks after injury until the end of the experiment at 9 weeks ($p < 0.05$ to 0.01, two-way ANOVA).

3.4. Combining PST/SC Transplantation with LV/PST Injection Does Not Lead to Elevated Pain Sensation

Since the over-expression of PSA in the spinal cord promotes the sprouting of axons in the spinal cord, aberrant sprouting of sensory axons might cause abnormal sensitivity to painful stimuli. In the current study, we used the manual Von Frey (VF) test for mechanical withdrawal thresholds and the Hargreaves test for noxious thermal sensitivity. Dorsal column transection axotomizes most of the ascending fibers for tactile perception. The VF test showed a significant increase in hindpaw withdrawal threshold at day 3 in both the GFP and PST groups (Figure 5B). The mechanical thresholds slightly recovered one week after surgery but remained at a significantly elevated level until the end of the experiment at 9 weeks after surgery. There is no significant difference in the mechanical thresholds between the PST and GFP groups during the entire period of the experiment, indicating that engineered PSA expression at the thoracic spinal cord plus PST/SC transplantation did not cause mechanical allodynia. Dorsal column transection at the T8 level did not cause a significant change in response to a thermal stimulus to the hindpaws and there

is no difference in thermal sensitivity between the PST and GFP groups (Figure 5C,D). The combined treatments of PST/SC transplantation and LV/PST injection to the thoracic spinal cord did not induce thermal hyperalgesia to noxious heat stimuli to the hindlimbs as the spinothalamic tract axons below the lesion site were intact.

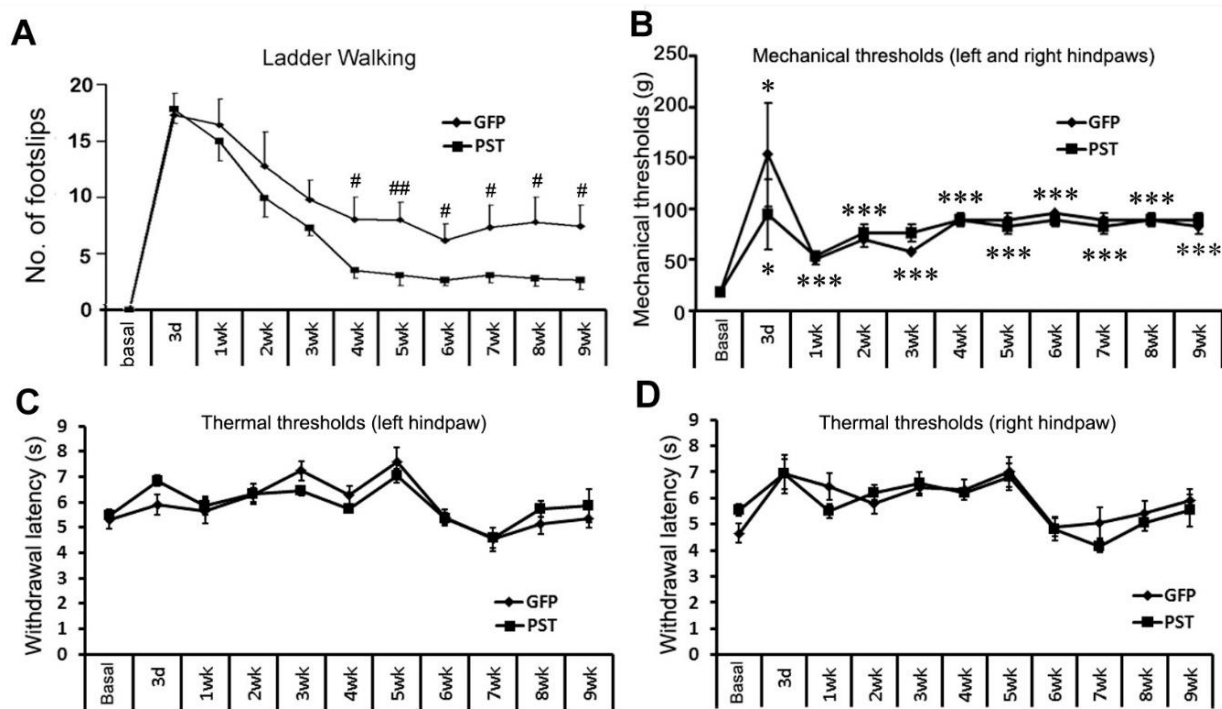


Figure 5. Motor and sensory functional tests. **(A)** Ladder crossing for motor functional test of the rat hindlimbs. The animals receiving transplantation of GFP/SCs plus LV/GFP injection made significantly more hindlimb slips while walking on the horizontal ladder in comparison with animals receiving transplantation of GFP and PST co-transduced SCs (GFP-PST/SCs) plus LV/PST injection. Data are presented as mean \pm SEM. # $p < 0.05$, ## $p < 0.01$, compared between PST and GFP groups, two-way ANOVA, $n = 7$. **(B)** Von Frey test for tactile perception of the hindpaws. Hindpaw withdrawal thresholds increased significantly at post-injury day 3 in both GFP and PST groups. The mechanical thresholds recovered slightly one week after surgery but remained at a significantly elevated level until the end of the experiment. There is no significant difference in the mechanical thresholds between the PST and GFP groups during the period of the experiment. Data are presented as mean \pm SEM. * $p < 0.05$, *** $p < 0.001$, compared with the base level before surgery (asterisks illustrating the statistical significance apply to both GFP and PST groups), two-way ANOVA, $n = 7$. **(C,D)** Hargreaves test for thermal nociception of hindpaws. Measurement of the mean latencies for thermal withdrawal thresholds of both hindpaws did not show significant changes to nociceptive thermal stimuli after dorsal column transection in both GFP and PST groups. There is also no significant difference in nociceptive thermal sensitivities between PST and GFP groups.

3.5. PST/SCs Maintain Their Capacity to Myelinate Axons

We examined the expression of peripheral myelin protein P0 as an indicator for myelination formed by SCs within the transplants (Figure 6). Although we showed the regenerating or sprouting CST axons did not grow deep into the SC transplants, other types of axons, such as serotonergic axons, can grow into the SC transplants (our unpublished data) [36,37]. P0 was highly expressed in GFP-PST/SCs (Figure 6A). Confocal images showed that GFP-PST/SCs (green in Figure 6D) and GFP/SCs (green in Figure 6E) formed P0⁺ internodes (red, arrowheads) around neurofilament⁺ axons (blue). Some P0⁺ internodes were formed by host SCs migrated into the transplants (arrows in Figure 6D,E). Calculation of the ratios of P0⁺/GFP⁺ internodes over GFP⁺ cells showed that the ratios were very close

for the GFP-PST/SCs and GFP/SCs (0.56 ± 0.02 vs. 0.55 ± 0.06 , $p = 0.78$), indicating that transplanted GFP-PST/SCs and GFP/SCs had a similar capacity of myelination. However, calculation of the ratios of P0⁺ cells (including both transplanted and host SCs migrated into the transplants) over P0⁺/GFP⁺ cells (representing transplanted GFP-PST/SCs or GFP/SCs) showed the ratio is much higher in the PST group than in the GFP group (2.7 ± 0.3 vs. 1.7 ± 0.2 , $p < 0.05$), indicating that there was increased migration and myelination from host SCs in the PST group.

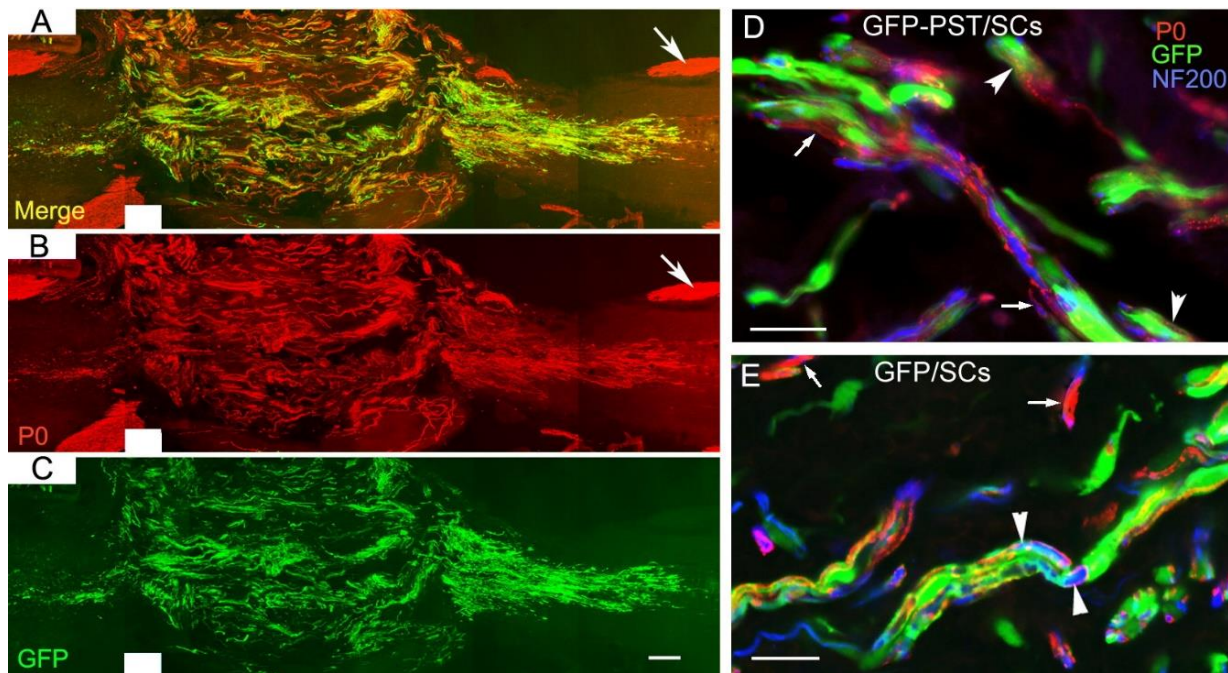


Figure 6. Expression of peripheral myelin marker P0 in transplanted Schwann cells. Spinal sections from animals killed 9 weeks after transplantation were immunostained for P0 and NF200. (A) Merged image showing the expression of P0 (red in (A,B)) and GFP (green in (A,C)) in GFP and PST co-transduced Schwann cell (GFP-PST/SCs) transplanted in the spinal cord. Arrows in (A,B) point to the P0 immunoreactivity in the spinal nerve roots. (D,E) Confocal images showing that transplanted GFP-PST/SCs (green in (D)) and GFP/SCs (green in (E)) formed P0⁺ internodes (red, arrowheads) around neurofilament⁺ axons (blue). Some P0⁺ internodes were formed by migrated host SCs (arrows). Scale bar = 200 μ m in (C), 20 μ m in (D,E).

4. Discussion

The results from the current study show that the combination of transplantation of PST/SCs into a spinal cord injury site with the engineered expression of PSA close to the lesion can promote significant growth and sprouting of CST axons, which was associated with faster and greater locomotor functional recovery. Myelination of CNS axons by transplanted GFP-PST/SCs was not hindered when checked 9 weeks post-transplantation. Furthermore, transplanted GFP-PST/SCs together with engineered PSA expression in the spinal cord facilitated the migration of host SCs into injured spinal cord, and SC transplants increased the myelination of the regenerating and sprouting CNS axons. In addition, we also show that GFP-PST/SC transplantation plus LV/PST injection to the host spinal cord did not cause mechanical allodynia or thermal hyperalgesia.

Although not directly comparable to the results reported by other groups due to the differences in species and strains of animals, viral vectors, injury models, and axon tracing method used, our strategy of combining GFP-PST/SC transplantation and engineered PSA expression showed higher efficacy in enhancing the regeneration of injured CST axons in comparison with either PST/SC transplantation alone [28] or the engineered

expression of PSA in spinal cord alone [25]. In our study, the number of BDA⁺ axonal profiles (including the branches of sprouting axons) counted at 4 mm caudal to the lesion border is 31% of the BDA⁺ axons counted at 8 mm rostral to the lesion. In the study by El Maarouf et al. [25], they performed the transection of the right CST on GFAP-TVA mice followed by transducing the lesioned spinal cord with a TVA-specific HIV vector to specifically transduce astrocytes. They found 10% of axons growing across the lesion, reached 0.5 mm in the caudal spinal cord, but failed to extend further. In the study by Ghosh et al. [28], they performed contusion injury to Fischer rats and transplanted PST/SCs into the lesion. They found many 5-HT axons and BDA-labelled CST axons growing into the transplants, and a number of BDA⁺ axons were able to grow to 1.5 mm caudal to the lesion. Since the method they used for the quantification of BDA-labelled axons is quite different from ours, it is difficult to directly compare the density of BDA⁺ axons in their study with ours. However, based on rough estimation, there were more BDA⁺ axons in the caudal spinal cord in our animals with combined GFP-PST/SC transplantation and engineered PSA expression than in their animals with PST/SC transplantation alone. The results confirm our hypothesis on the synergistic effect of combining GFP-PST/SC transplantation and engineered PSA expression in the spinal cord.

In our study, we observed locomotor functional recovery in both the GFP and PST groups soon after the dorsal column transection, which could not be attributed to axonal regeneration. Apart from recovery from spinal shock, spontaneous axonal sprouting from intact dorsolateral and ventral CST axons and axons from other motor tracts such as descending serotonergic pathways might play an important role in functional recovery. Collateral sprouting of intact CST axons in the ventral and dorsolateral columns has been reported to contribute to spontaneous functional recovery in mouse and rat spinal cord injury models [38]. Serotonergic axons, descending in the ventral and lateral columns of the spinal cord and modulating the excitability of spinal cord circuits, are capable of initiating and controlling rhythmic coordinated movements [39]. Our approach of combined treatments is likely to enhance spontaneous axonal sprouting and promote functional recovery. Spontaneous axonal sprouting after spinal cord injury has been shown to be associated with increased expression of PSA after spinal cord injury [14]. In an *in vitro* study, neurons were shown to grow longer neurites and have more branches when growing on PSA-expressing HeLa cells [40,41]. Engineered expression of PSA in the injured spinal cord should facilitate the sprouting of intact axons. In the longer term after injury, regeneration of injured axons may also contribute to the observed functional recovery. We showed here that the number of CST axonal profiles in the caudal grey matter was closely correlated with the number of spared CST axons in the GFP group, indicating that the CST axonal profiles in the caudal spinal cord are due to collateral sprouting of intact CST axons rather than the regeneration of injured CST axons. However, in the PST group, the increased number of BDA⁺ axons in the caudal grey matter was not correlated with the number of spared CST axons, implicating that the increased number of BDA⁺ axons was due to increased sprouting from both intact and injured CST axons.

The schematic drawings in Figure 7 illustrate the effects of our combinatory strategy: engineered PSA expression around the lesion made the glial scar and the spinal cord less inhibitory for the growth and sprouting of the regenerating and intact axons, while GFP-PST/SC transplants filled the lesion cavity and provided a permissive cellular bridge for regenerating CST axons. The growth and sprouting of serotonergic axons are not shown, although they may contribute to the locomotor functional recovery.

One concern on enhancing axonal sprouting by engineered PSA expression in the spinal cord is that it may potentially cause aberrant sprouting of primary afferents and lead to heightened pain states. Nevertheless, we showed that there was no mechanical allodynia or thermal hyperalgesia in the PST group compared with the GFP control group. It has been reported that the presence of PSA in the dorsal spinal cord allows the modification or uncoupling of spinal cord nociceptive synapses in response to chronic pain [42]. Engineered expression of PSA may actively prevent excessive pathological input. This indicates that

the expression of PSA has multifaceted functions in promoting the repair of the injured spinal cord.

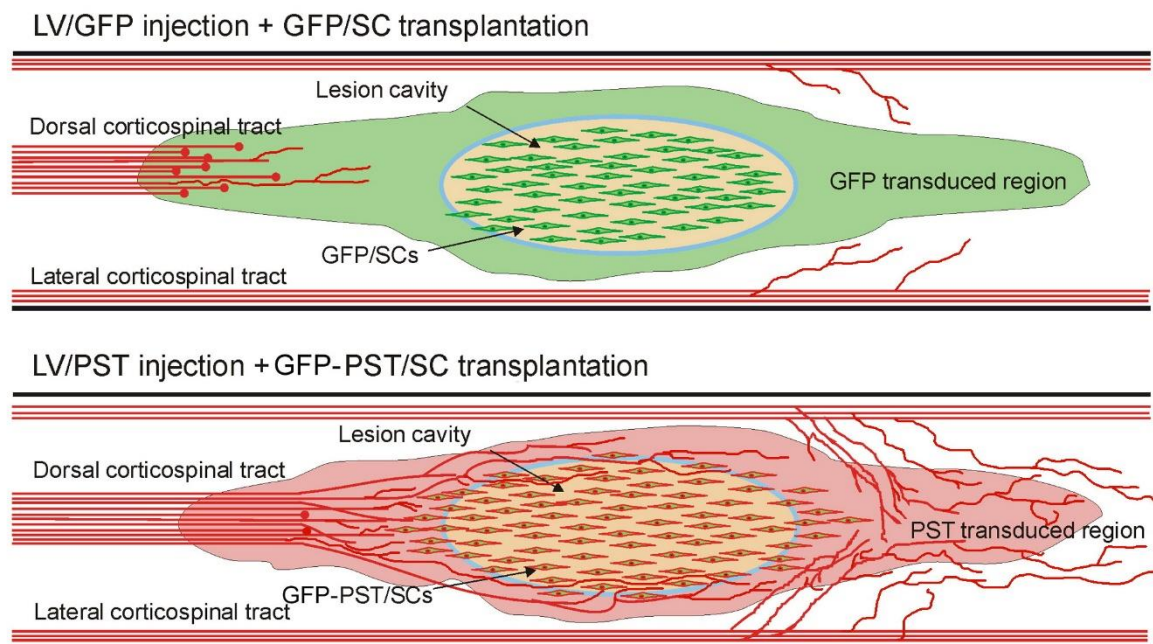


Figure 7. Schematic diagram showing the effects of combined transplantation of GFP- or PST-transduced Schwann cells with intraspinal injection of LV/GFP or LV/PST in promoting corticospinal tract axon regeneration and sprouting.

The myelination of CNS axons is also crucial for functional recovery. Since PSA acts like a spacer and reduces cell adhesion, it is reasonable to predict that PSA on SCs may affect myelination. It has been reported that down-regulation of PSA on oligodendrocytes is required for efficient myelin formation [43]. In the current study, we confirmed that implanted GFP-PST/SCs had unimpaired myelination potential, in agreement with previous *in vitro* [26] and *in vivo* studies [27,29]. We found engineered PSA expression in the host spinal cord plus GFP-PST/SC transplantation increased the expression of P0 protein by host SCs inside the transplants, indicating enhanced migration of host SCs into the lesion site, which further confirms our previous finding that engineered expression of PSA in the spinal cord increased the migration of both endogenous SCs and transplanted SCs along the PSA positive pathway [10,23]. A possible reason that PSA on SCs did not affect myelination in our study is that by 9 weeks post-transplantation, the level of PSA expression on the transplanted SCs had dropped significantly. Another likely reason is that the surface area of the myelin sheath of a myelinating SC is 100 times that of an unmyelinated SC; therefore, the density of PSA molecules on the SC membrane would be significantly reduced.

In conclusion, this study shows that the combination of engineered expression of PSA in the lesioned spinal cord with the transplantation of PST/SCs promotes the regeneration and sprouting of CST axons and enhances the migration of host SCs into the lesion, which leads to long-lasting motor functional recovery without inducing allodynia or hyperalgesia. Such a combined gene- and cell-based therapeutic strategy proves to be more effective in promoting axonal regeneration than single treatments. Combination with additional approaches, such as activation of the regeneration mechanism of injured neurons by delivery of neurotrophic factors and other signalling molecules [44–47], or manipulation of the intracellular signalling pathways [48,49], or degrading extracellular inhibitory molecules [50], may achieve even more significant axonal regeneration and functional recovery.

Author Contributions: Conceptualization and methodology, Y.Z. and X.B.; data generation, F.G., Y.Z., D.W., J.L. and S.G.; original draft preparation, review, and editing, X.B.; funding acquisition, Y.Z. and X.B. All authors have read and agreed to the published version of the manuscript.

Funding: This research was funded by the Wellcome Trust (grant number: 065412).

Institutional Review Board Statement: Not applicable.

Informed Consent Statement: Not applicable.

Data Availability Statement: All data are provided herein.

Acknowledgments: We thank John V. Priestley for the critical reading of the manuscript.

Conflicts of Interest: The authors declare no conflict of interest.

References

- O'Shea, T.M.; Burda, J.E.; Sofroniew, M.V. Cell biology of spinal cord injury and repair. *J. Clin. Investig.* **2017**, *127*, 3259–3270. [[CrossRef](#)]
- Assinck, P.; Duncan, G.J.; Hilton, B.J.; Plemel, J.R.; Tetzlaff, W. Cell transplantation therapy for spinal cord injury. *Nat. Neurosci.* **2017**, *20*, 637–647. [[CrossRef](#)] [[PubMed](#)]
- Ramalho, B.D.S.; de Almeida, F.M.; Martinez, A.M.B. Cell therapy and delivery strategies for spinal cord injury. *Histol. Histopathol.* **2021**, *36*, 907–920. [[PubMed](#)]
- Deng, L.X.; Walker, C.; Xu, X.M. Schwann cell transplantation and descending propriospinal regeneration after spinal cord injury. *Brain Res.* **2015**, *1619*, 104–114. [[CrossRef](#)]
- Monje, P.V.; Deng, L.; Xu, X.M. Human Schwann Cell Transplantation for Spinal Cord Injury: Prospects and Challenges in Translational Medicine. *Front. Cell. Neurosci.* **2021**, *15*, 690894. [[CrossRef](#)] [[PubMed](#)]
- Anderson, K.D.; Guest, J.D.; Dietrich, W.D.; Bartlett Bunge, M.; Curiel, R.; Dididze, M.; Green, B.A.; Khan, A.; Pearse, D.D.; Saraf-Lavi, E.; et al. Safety of Autologous Human Schwann Cell Transplantation in Subacute Thoracic Spinal Cord Injury. *J. Neurotrauma* **2017**, *34*, 2950–2963. [[CrossRef](#)]
- Zhou, X.H.; Ning, G.Z.; Feng, S.Q.; Kong, X.H.; Chen, J.T.; Zheng, Y.F.; Ban, D.X.; Liu, T.; Li, H.; Wang, P. Transplantation of autologous activated Schwann cells in the treatment of spinal cord injury: Six cases, more than five years of follow-up. *Cell Transplant.* **2012**, *21* (Suppl. S1), S39–S47. [[CrossRef](#)]
- Saberi, H.; Moshayedi, P.; Aghayan, H.R.; Arjmand, B.; Hosseini, S.K.; Emami-Razavi, S.H.; Rahimi-Movaghar, V.; Raza, M.; Firouzi, M. Treatment of chronic thoracic spinal cord injury patients with autologous Schwann cell transplantation: An interim report on safety considerations and possible outcomes. *Neurosci. Lett.* **2008**, *443*, 46–50. [[CrossRef](#)]
- Gant, K.L.; Guest, J.D.; Palermo, A.E.; Vedantam, A.; Jimshelishvili, G.; Bunge, M.B.; Brooks, A.E.; Anderson, K.D.; Thomas, C.K.; Santamaria, A.J.; et al. Phase 1 Safety Trial of Autologous Human Schwann Cell Transplantation in Chronic Spinal Cord Injury. *J. Neurotrauma* **2022**, *39*, 285–299. [[CrossRef](#)]
- Luo, J.; Bo, X.; Wu, D.; Yeh, J.; Richardson, P.M.; Zhang, Y. Promoting survival, migration, and integration of transplanted Schwann cells by over-expressing polysialic acid. *Glia* **2011**, *59*, 424–434. [[CrossRef](#)] [[PubMed](#)]
- Cregg, J.M.; DePaul, M.A.; Filous, A.R.; Lang, B.T.; Tran, A.; Silver, J. Functional regeneration beyond the glial scar. *Exp. Neurol.* **2014**, *253*, 197–207. [[CrossRef](#)] [[PubMed](#)]
- Clifford, T.; Finkel, Z.; Rodriguez, B.; Joseph, A.; Cai, L. Current Advancements in Spinal Cord Injury Research-Glial Scar Formation and Neural Regeneration. *Cells* **2023**, *12*, 853. [[CrossRef](#)] [[PubMed](#)]
- Dusart, I.; Morel, M.P.; Wehrle, R.; Sotelo, C. Late axonal sprouting of injured Purkinje cells and its temporal correlation with permissive changes in the glial scar. *J. Comp. Neurol.* **1999**, *408*, 399–418. [[CrossRef](#)]
- Camand, E.; Morel, M.P.; Faissner, A.; Sotelo, C.; Dusart, I. Long-term changes in the molecular composition of the glial scar and progressive increase of serotonergic fibre sprouting after hemisection of the mouse spinal cord. *Eur. J. Neurosci.* **2004**, *20*, 1161–1176. [[CrossRef](#)] [[PubMed](#)]
- Rutishauser, U. Polysialic acid in the plasticity of the developing and adult vertebrate nervous system. *Nat. Rev. Neurosci.* **2008**, *9*, 26–35. [[CrossRef](#)]
- Schnaar, R.L.; Gerardy-Schahn, R.; Hildebrandt, H. Sialic acids in the brain: Gangliosides and polysialic acid in nervous system development, stability, disease, and regeneration. *Physiol. Rev.* **2014**, *94*, 461–518. [[CrossRef](#)]
- Seki, T.; Arai, Y. Distribution and possible roles of the highly polysialylated neural cell adhesion molecule (NCAM-H) in the developing and adult central nervous system. *Neurosci. Res.* **1993**, *17*, 265–290. [[CrossRef](#)]
- Kiss, J.Z.; Muller, D. Contribution of the neural cell adhesion molecule to neuronal and synaptic plasticity. *Rev. Neurosci.* **2001**, *12*, 297–310. [[CrossRef](#)]
- Zhang, Y.; Yeh, J.; Richardson, P.M.; Bo, X. Cell adhesion molecules of the immunoglobulin superfamily in axonal regeneration and neural repair. *Restor. Neurol. Neurosci.* **2008**, *26*, 81–96.
- El Maarouf, A.; Rutishauser, U. Use of PSA-NCAM in repair of the central nervous system. *Adv. Exp. Med. Biol.* **2010**, *663*, 137–147.

21. Eckhardt, M.; Muhlenhoff, M.; Bethe, A.; Koopman, J.; Frosch, M.; Gerardy-Schahn, R. Molecular characterization of eukaryotic polysialyltransferase-1. *Nature* **1995**, *373*, 715–718. [[CrossRef](#)]
22. Angata, K.; Suzuki, M.; Fukuda, M. Differential and cooperative polysialylation of the neural cell adhesion molecule by two polysialyltransferases, PST and STX. *J. Biol. Chem.* **1998**, *273*, 28524–28532. [[CrossRef](#)]
23. Zhang, Y.; Zhang, X.; Wu, D.; Verhaagen, J.; Richardson, P.M.; Yeh, J.; Bo, X. Lentiviral-mediated expression of polysialic acid in spinal cord and conditioning lesion promote regeneration of sensory axons into spinal cord. *Mol. Ther.* **2007**, *15*, 1796–1804. [[CrossRef](#)]
24. Zhang, Y.; Ghadiri-Sani, M.; Zhang, X.; Richardson, P.M.; Yeh, J.; Bo, X. Induced expression of polysialic acid in the spinal cord promotes regeneration of sensory axons. *Mol. Cell. Neurosci.* **2007**, *35*, 109–119. [[CrossRef](#)] [[PubMed](#)]
25. El Maarouf, A.; Petridis, A.K.; Rutishauser, U. Use of polysialic acid in repair of the central nervous system. *Proc. Natl. Acad. Sci. USA* **2006**, *103*, 16989–16994. [[CrossRef](#)]
26. Lavdas, A.A.; Franceschini, I.; Dubois-Dalcq, M.; Matsas, R. Schwann cells genetically engineered to express PSA show enhanced migratory potential without impairment of their myelinating ability in vitro. *Glia* **2006**, *53*, 868–878. [[CrossRef](#)] [[PubMed](#)]
27. Bachelin, C.; Zujovic, V.; Buchet, D.; Mallet, J.; Baron-Van Evercooren, A. Ectopic expression of polysialylated neural cell adhesion molecule in adult macaque Schwann cells promotes their migration and remyelination potential in the central nervous system. *Brain* **2010**, *133*, 406–420. [[CrossRef](#)] [[PubMed](#)]
28. Ghosh, M.; Tuesta, L.M.; Puentes, R.; Patel, S.; Melendez, K.; El Maarouf, A.; Rutishauser, U.; Pearse, D.D. Extensive cell migration, axon regeneration, and improved function with polysialic acid-modified Schwann cells after spinal cord injury. *Glia* **2012**, *60*, 979–992. [[CrossRef](#)]
29. Papastefanaki, F.; Chen, J.; Lavdas, A.A.; Thomaidou, D.; Schachner, M.; Matsas, R. Grafts of Schwann cells engineered to express PSA-NCAM promote functional recovery after spinal cord injury. *Brain* **2007**, *130*, 2159–2174. [[CrossRef](#)]
30. Angata, K.; Yen, T.Y.; El-Battari, A.; Macher, B.A.; Fukuda, M. Unique disulfide bond structures found in ST8Sia IV polysialyltransferase are required for its activity. *J. Biol. Chem.* **2001**, *276*, 15369–15377. [[CrossRef](#)]
31. Dull, T.; Zufferey, R.; Kelly, M.; Mandel, R.J.; Nguyen, M.; Trono, D.; Naldini, L. A third-generation lentivirus vector with a conditional packaging system. *J. Virol.* **1998**, *72*, 8463–8471. [[CrossRef](#)]
32. Brockes, J.P.; Fields, K.L.; Raff, M.C. Studies on cultured rat Schwann cells. I. Establishment of purified populations from cultures of peripheral nerve. *Brain Res.* **1979**, *165*, 105–118. [[CrossRef](#)] [[PubMed](#)]
33. Neafsey, E.J.; Bold, E.L.; Haas, G.; Hurley-Gius, K.M.; Quirk, G.; Sievert, C.F.; Terreberry, R.R. The organization of the rat motor cortex: A microstimulation mapping study. *Brain Res.* **1986**, *396*, 77–96. [[CrossRef](#)] [[PubMed](#)]
34. Hargreaves, K.; Dubner, R.; Brown, F.; Flores, C.; Joris, J. A new and sensitive method for measuring thermal nociception in cutaneous hyperalgesia. *Pain* **1988**, *32*, 77–88. [[CrossRef](#)]
35. Chaplan, S.R.; Bach, F.W.; Pogrel, J.W.; Chung, J.M.; Yaksh, T.L. Quantitative assessment of tactile allodynia in the rat paw. *J. Neurosci. Methods* **1994**, *53*, 55–63. [[CrossRef](#)]
36. Enomoto, M.; Bunge, M.B.; Tsoulfas, P. A multifunctional neurotrophin with reduced affinity to p75NTR enhances transplanted Schwann cell survival and axon growth after spinal cord injury. *Exp. Neurol.* **2013**, *248*, 170–182. [[CrossRef](#)]
37. Lavdas, A.A.; Chen, J.; Papastefanaki, F.; Chen, S.; Schachner, M.; Matsas, R.; Thomaidou, D. Schwann cells engineered to express the cell adhesion molecule L1 accelerate myelination and motor recovery after spinal cord injury. *Exp. Neurol.* **2010**, *221*, 206–216. [[CrossRef](#)] [[PubMed](#)]
38. Steward, O.; Zheng, B.; Tessier-Lavigne, M.; Hofstadter, M.; Sharp, K.; Yee, K.M. Regenerative growth of corticospinal tract axons via the ventral column after spinal cord injury in mice. *J. Neurosci.* **2008**, *28*, 6836–6847. [[CrossRef](#)] [[PubMed](#)]
39. Ghosh, M.; Pearse, D.D. The role of the serotonergic system in locomotor recovery after spinal cord injury. *Front. Neural Circuits* **2014**, *8*, 151. [[CrossRef](#)]
40. Nakayama, J.; Fukuda, M.N.; Fredette, B.; Ranscht, B.; Fukuda, M. Expression cloning of a human polysialyltransferase that forms the polysialylated neural cell adhesion molecule present in embryonic brain. *Proc. Natl. Acad. Sci. USA* **1995**, *92*, 7031–7035. [[CrossRef](#)]
41. Angata, K.; Nakayama, J.; Fredette, B.; Chong, K.; Ranscht, B.; Fukuda, M. Human STX polysialyltransferase forms the embryonic form of the neural cell adhesion molecule. Tissue-specific expression, neurite outgrowth, and chromosomal localization in comparison with another polysialyltransferase, PST. *J. Biol. Chem.* **1997**, *272*, 7182–7190. [[CrossRef](#)] [[PubMed](#)]
42. El Maarouf, A.; Kolesnikov, Y.; Pasternak, G.; Rutishauser, U. Polysialic acid-induced plasticity reduces neuropathic insult to the central nervous system. *Proc. Natl. Acad. Sci. USA* **2005**, *102*, 11516–11520. [[CrossRef](#)]
43. Fewou, S.N.; Ramakrishnan, H.; Bussow, H.; Gieselmann, V.; Eckhardt, M. Down-regulation of polysialic acid is required for efficient myelin formation. *J. Biol. Chem.* **2007**, *282*, 16700–16711. [[CrossRef](#)]
44. Zhang, Y.; Dijkhuizen, P.A.; Anderson, P.N.; Lieberman, A.R.; Verhaagen, J. NT-3 delivered by an adenoviral vector induces injured dorsal root axons to regenerate into the spinal cord of adult rats. *J. Neurosci. Res.* **1998**, *54*, 554–562. [[CrossRef](#)]
45. Kadoya, K.; Tsukada, S.; Lu, P.; Coppola, G.; Geschwind, D.; Filbin, M.T.; Blesch, A.; Tuszynski, M.H. Combined intrinsic and extrinsic neuronal mechanisms facilitate bridging axonal regeneration one year after spinal cord injury. *Neuron* **2009**, *64*, 165–172. [[CrossRef](#)] [[PubMed](#)]
46. Leibinger, M.; Zeitler, C.; Gobrecht, P.; Andreadaki, A.; Gisselmann, G.; Fischer, D. Transneuronal delivery of hyper-interleukin-6 enables functional recovery after severe spinal cord injury in mice. *Nat. Commun.* **2021**, *12*, 391. [[CrossRef](#)] [[PubMed](#)]

47. Wu, D.; Lee, S.; Luo, J.; Xia, H.; Gushchina, S.; Richardson, P.M.; Yeh, J.; Krügel, U.; Franke, H.; Zhang, Y.; et al. Intraneural Injection of ATP Stimulates Regeneration of Primary Sensory Axons in the Spinal Cord. *J. Neurosci.* **2018**, *38*, 1351–1365. [[CrossRef](#)]
48. Wu, D.; Yang, P.; Zhang, X.; Luo, J.; Haque, M.E.; Yeh, J.; Richardson, P.M.; Zhang, Y.; Bo, X. Targeting a dominant negative rho kinase to neurons promotes axonal outgrowth and partial functional recovery after rat rubrospinal tract lesion. *Mol. Ther.* **2009**, *17*, 2020–2030. [[CrossRef](#)]
49. Hannila, S.S.; Filbin, M.T. The role of cyclic AMP signaling in promoting axonal regeneration after spinal cord injury. *Exp. Neurol.* **2008**, *209*, 321–332. [[CrossRef](#)]
50. Kanno, H.; Pressman, Y.; Moody, A.; Berg, R.; Muir, E.M.; Rogers, J.H.; Ozawa, H.; Itoi, E.; Pearse, D.D.; Bunge, M.B. Combination of engineered Schwann cell grafts to secrete neurotrophin and chondroitinase promotes axonal regeneration and locomotion after spinal cord injury. *J. Neurosci.* **2014**, *34*, 1838–1855. [[CrossRef](#)]

Disclaimer/Publisher’s Note: The statements, opinions and data contained in all publications are solely those of the individual author(s) and contributor(s) and not of MDPI and/or the editor(s). MDPI and/or the editor(s) disclaim responsibility for any injury to people or property resulting from any ideas, methods, instructions or products referred to in the content.